

Automated segmentation method for the 3-D ultrasound carotid image based on the Geometrically deformable model with automatic merge function

Xiang Li, Zigang Wang, Hongbing Lu and Zhengrong Liang
Department of Radiology, State University of New York at Stony Brook, NY 11794

ABSTRACT

Stenosis of the carotid is the most common cause of the stroke. The accurate measurement of the volume of the carotid and visualization of its shape are helpful in improving diagnosis and minimizing the variability of assessment of the carotid disease. Due to the complex anatomic structure of the carotid, it is mandatory to define the initial contours in every slice, which is very difficult and usually requires tedious manual operations. The purpose of this paper is to propose an automatic segmentation method, which automatically provides the contour of the carotid from the 3-D ultrasound image and requires minimum user interaction. In this paper, we developed the Geometrically Deformable Model (GDM) with automatic merge function. In our algorithm, only two initial contours in the topmost slice and four parameters are needed in advance. Simulated 3-D ultrasound image was used to test our algorithm. 3-D display of the carotid obtained by our algorithm showed almost identical shape with true 3-D carotid image. In addition, experimental results also demonstrated that error of the volume measurement of the carotid based on the three different initial contours is less than 1% and its speed was a very fast.

Keywords: automated segmentation, geometrically deformable model, contour deformation

1.INTRODUCTION

Stenosis of the carotid is the most common cause of the stroke, which is the leading cause of the death after the cardiovascular diseases and cancers [1,2]. The accurate measurement of the volume of the carotid and visualization of its shape are helpful in improving diagnosis and minimizing the variability of assessment of the carotid disease. To do this, the precise delineation of the contour of the carotid is necessary. The active contour model, first introduced by Kass et al and also called snake model, was widely used in the medical imaging processing [3,4,5]. This method defines the contour as a series of connected spline segments and requires the initiation of so many parameters. At this point, another model, geometrically deformable model (GDM) introduced by Lobregt et al, which is somewhat different from conventional snake model, has an obvious advantage of simplicity and less parameter setting [6,7,8]. Unfortunately, these two models do not have the ability of automatic merge function of the multiple contours. It is well known that the carotid consists of common carotid, internal carotid and external carotid, which mean that there should be two contours in some slices and a contour in other slices. Due to this kind of complex anatomic structure of the carotid, it is mandatory to define the initial contours in every slice for the conventional active contour model, which is very difficult and usually requires tedious manual operations. In addition, another drawback of this kind of method is that the initial contour close to the true boundary must be provided in order to achieve good final results [9]. The purpose of this paper is to propose an automatic segmentation method, which based on the GDM but automatically provides the contour of the carotid from the 3-D ultrasound image and requires minimum user interaction. In our algorithm, only two initial contours and four parameters are needed.

2.METHODS

Geometrically Deformable Model

Geometrically deformable model, which was first introduced by Miller et al, was refined by Lobregt et al. For the GDM model, the contour is defined as a series of vertices, which are connected by straight line. This model can be

regard as discrete active contour model. During the deformation process of the contour, unlike conventional active contour model, just vertices were able to deform. In this paper, we adopted the GDM described by Lobregt et al.

The main idea of the GDM is that the internal force of contour is used to describe the smoothness constraint and external force of contour is applied to depict the attraction of boundary, the total force function is defined as the weighting sum of both internal and external force of the contour. The process of contour evolving to the final contour is the minimizing process of the total force function. Followings are how to design internal, external and total force function and how to minimize the total force function to obtain the final contour in this paper.

In this paper, the contour is defined as the series of vertices along the clockwise direction, as can be seen in figure1. The internal force is described as the convolution of filter function and the curvature of the vertices. The main purpose of introducing internal force is to minimize the local curvature and obtain the smooth final contour. In order to define the internal and external force, we must define the local radial unit vector in advance.

$$\vec{r}_i = \frac{\vec{d}_i - \vec{d}_{i-1}}{\|\vec{d}_i - \vec{d}_{i-1}\|} \quad (1)$$

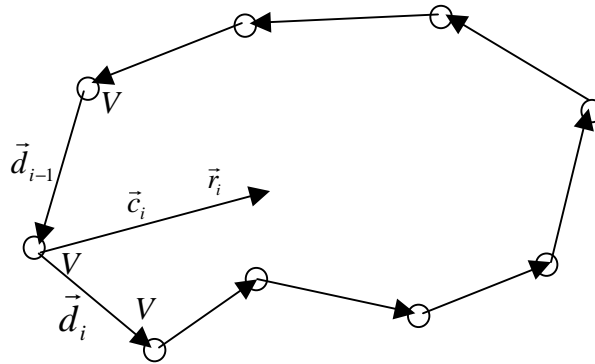


Figure1. The Geometrically deformable model and the definition of the local curvature

The local curvature at the vertex $V_i(x_i, y_i)$ is defined as the differences between the adjacent vectors drawn in the figure1.

$$\vec{c}_i = \vec{d}_i - \vec{d}_{i-1} \quad (2)$$

According to the equation (2), we can find out that the curvature vector has a same direction as the local radial vector. The aim of introducing the filter function is to prevent the shrinking phenomenon. In this paper, we adopted the same filter function as Lobregt and Zahalka [7,8].

$$k_i = \{\dots, 0, 0, -\frac{1}{2}, 1, -\frac{1}{2}, 0, 0, \dots\} \quad (3)$$

Therefore, the internal force at the vertex V_i can be described as following equation:

$$F_{in,i} = (-\frac{1}{2}\|c_{i-1}\| + \|c_i\| - \frac{1}{2}\|c_{i+1}\|) \cdot \vec{r}_i \quad (4)$$

The external force provides the driving force for the deformation of the contour to the final contour and represents the some kind of image features. Usually, the gradient information is the most popular image feature for the active contour model and GDM. In this work we also adopted this information to define the external force at the vertex V_i .

$$F_{ex,i} = (-\nabla E \cdot \vec{r}_i) \cdot \vec{r}_i \quad (5)$$

Here, we just adopted the radial component of the gradient $-\nabla E$ to avoid the clustering phenomenon. The Sobel operator is used to calculate the local gradient vector. Therefore, we can easily obtain the total force of the contour:

$$F_{total} = \omega_{in} \sum_i F_{in,i} + \omega_{ex} \sum_i F_{ex,i} \quad (6)$$

Where the parameter ω_{in}, ω_{ex} are the weighting factor of the internal force and external force, respectively. The larger value of ω_{in} has a tendency to keep the contour smoothing and larger value of ω_{ex} makes contour closer to the true boundary.

Deformation process

The deformation process of the contour is the process minimizing the total force function. In this work, we adopted vertex by vertex minimization strategy. Here, we also define another parameter d , which means the searching distance from the present pixel. According to the above definitions, we know that every vertex deform along the local radial direction. As can be seen in the figure2, for the present vertex V_i , it will move to another position V'_i , which is within d from present vertex and makes the total force of the new contour get minimum value. The appropriate setting of the parameter d is helpful accelerating the convergence speed and overcoming the drawback that initial contour must closer to the true boundary. During the deformation process, we also adopted the strategy of Lobregt, which restrict the distance between the adjacent vertices within the some scope. We used the parameter ω_{res} representing spatial resolution of the contour. In this work, if the distance between the adjacent vertices is large than the 1.5 times of the parameter ω_{res} , then the new vertex will be inserted between these adjacent vertices. If the distance between the adjacent vertices is less than the half of the parameter ω_{res} , then this vertex will be discarded. In addition, in order to avoid the clustering phenomenon further, we also confined the angle between adjacent vectors \vec{d}_i, \vec{d}_{i-1} is larger than $\pi/2$. This method can overcome clustering phenomenon very well, but sometimes it will blur sharp contour.

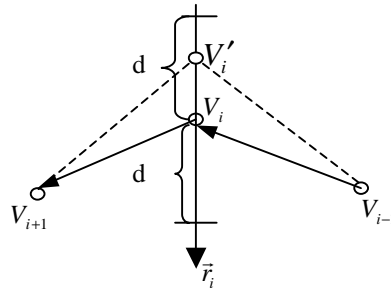


Figure2. The sketch of the deformation process of the contour

Automatic merge of the two contours

The carotid consists of common carotid, internal carotid and external carotid. In our work, 3-D ultrasound carotid image data was obtained from top to bottom, i.e. the common carotid is scanned after the other two parts. The basic idea of our automatically segmentation algorithm is to utilize two initial contours specified by the user in the topmost slice to calculate the final contours of the internal and external carotid in this slice and use these final contours as the initial contours for the next slice, and repeat this procedure slice by slice until the last one. Before a particular slice, in which two contours of the internal and external carotids will merge into one contour of the common carotid, the conventional GDM is able to carry out this contour evolving process. When encountering transition from internal and external carotid into common carotid, following criteria were used to judge if perform contour merge: the distance between internal carotid and external carotid in the same slice, the mean intensity and mean gradient value of each contour, the intensity and gradient of the regional contour. When the distance between internal and external carotid is larger than 2, the two contours of internal carotid and external carotid definitely are separated. If this distance is less than 2, we need to calculate the mean intensity and mean gradient value of each contour, the intensity and gradient of the regional contour. Here, the calculation of the mean intensity and gradient value of each contour not only based on the vertex of the contour, but also included these pixels of the straight line connected adjacent vertex. The regional contour means what

of one contour is very close to another contour (The distance must be less than 2). When the following conditions are satisfied simultaneously:

1. The distance between the two contours is less than 2.
2. The mean intensity of the regional contour less than mean intensity of the whole contour/4
3. The mean gradient of the regional contour less than mean gradient of the whole contour/4

Then the vertices with the regional contour will be removed. Finally, we have to rearrange the rest of vertices of the two contours along the clockwise direction to construct a one contour. Based on this contour, then we used GDM algorithm again to find the contour of the common carotid.

In summary, for our algorithm, the users need to set up four parameters: search scope, spatial resolution, weighting factors of the external and internal forces. During the minimization of the total force function, the search scope parameter confines the searching distance from a current vertex to any particular pixel on the curvature direction or anti-direction of this vertex, which allows our GDM model support bi-direction deformation and the fast convergence speed. The function of the last three parameters was mentioned in many literatures. In addition, the users have to provide two initial contours as the boundary of the internal and external carotid. During the deformation process, at a particular moment, in which two contours of the internal and external carotids will automatically merge into one contour of the common carotid.

Finally, by using the final contours of the carotid, we can calculate the volume of the carotid and display its 3-D image with surface rendering technique.

3.RESULTS

Simulation

In this work, we used simulated 3-D ultrasound images to evaluate our proposed algorithm. The image size was set up to 256x256x128. In the simulated images the gray value of 60 represents the carotid region and the gray value of 120 represents the background region. Then the white noises range from -40 to 40 are added into the image. The circles with different radius are used to represent the internal, external and common carotid.

Automatic merge function

Let us test our automatic merge strategy. The figure3a and figure 3c are adjacent slice image. It is clear that there are just internal and external carotid in the figure3a and transition from internal and external carotid to the common carotid in the figure3c. Therefore, two contours must merge into one from figure3a to figure3c. First, we provided two initial contours in the figure 3a, GDM is used to search final boundary as white circle in the figure3a. We uses them as initial contours for the next slice image. Figure 3b shows the intermediate process of the contours deformation. For this example, the difference between two contours should be zero, so automatic merge process has to be performed. Sometimes we also find that there is not intersection between these two contours based on different initial contours at same situation even though. Therefore, in order to enhance the robustness of the algorithm, we adopted the above condition1 instead of zero distance. Our automatic merge strategy is applied to judge whether perform merge operation and how to merge two contours into one contour. Figure 3c display the result of this strategy and demonstrate that our automatic merge strategy is very successful.

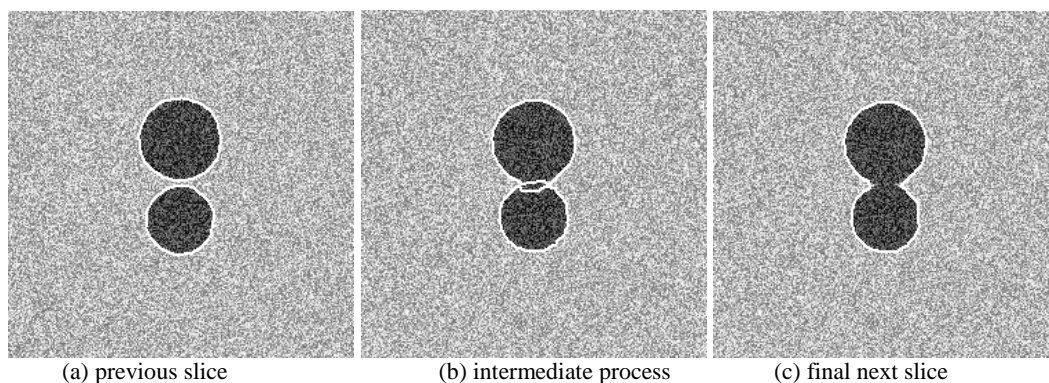


Figure3. The schematic diagram of the automatic merge process

Figure4 shows the three-dimension carotid image. For the topmost slice image, we give two initial contours for the internal and external carotid. The four parameters are set up as following:

$$\omega_{in} = 1, \omega_{ex} = 1, \omega_{re} = 3, d = 15 \quad (7)$$

Our automatic segmentation method is used to automatically produce the final contour of the whole carotid. Then we utilize surface rendering technique to produce 3-D carotid image. Figure 4a (a) is true carotid image based on the true boundary and figure 4b is the carotid image based on the boundary obtained by our automatic segmentation method. 3-D display of the carotid obtained by our algorithm showed almost identical shape with true 3-D carotid image.

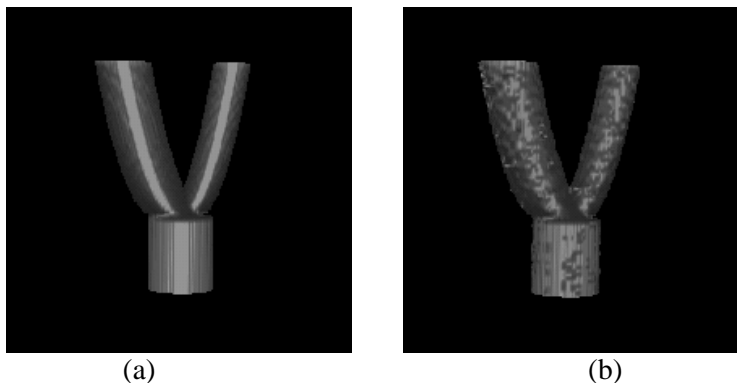


Figure 4. 3-D carotid image. Left (a) is true carotid image based on the true boundary, right (b) is the carotid image based on the boundary obtained by our automatic segmentation method.

Finally, we analyzed the influence of the different initial condition on the final results. As can be seen in figure5, we provide three different initial contours: from left to right, inside the true boundary, outside the true boundary and intersection with the true boundary, respectively. Table 1 show the results of the volume measurement based on the different initial contour by using our automatic segmentation method. The simulation experimental results show that the error of the volume measurement of the carotid based on the three different initial contours is less that 1%. This also demonstrated that our proposed segmentation method is robust for the setting of initial contour and support bi-direction deformation.

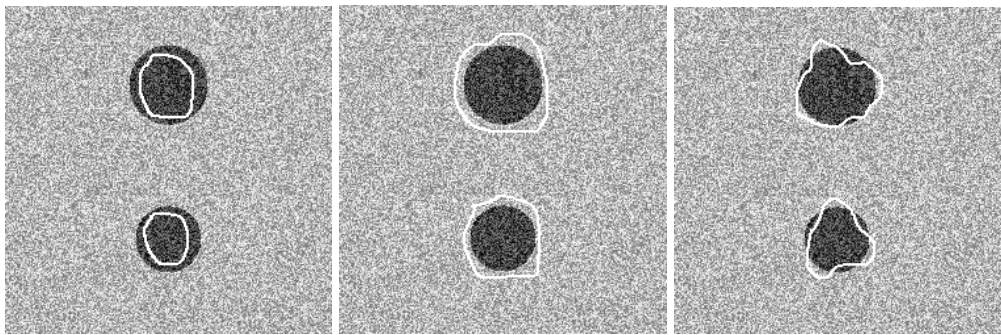


Figure5. Different initial contours.

Table. Accuracy of the volume measurement based on the different initial contour

	Volume (pixel)	Error
True Contour (TC)	252007	
Inside TC	253565	0.618%
Outside TC	253478	0.583%
Intersection with TC	253571	0.621%

In addition, the speed of our automatic segmentation method is also very fast. For this simulation, the total computing time is approximately 25 seconds for 256x256x128 image on a PC/400 Mhz pentium II with 256M RAM.

4.CONCLUSION

In this paper, the automated segmentation algorithm of 3-D ultrasound carotid image was developed and evaluated with simulated 3-D ultrasound image. The results indicate that automatic merge strategy of the contours is a successful and the algorithm is an efficient and robust for the different initial contours. However, there are also some limitations for our method. First, our segmentation method just supports this situation that the number of contour is known in advance like carotid image. It does not work on the indefinite number of contour. Second, the property of the GDM determined that it is not good in the corner situation, so this method does not support too complicated structure.

ACKNOWLEDGEMENTS

REFERENCE

1. V.Hachinski, "Brain attack", in *Physicians Guide to Stroke Diagnosis, Treatment, and prevention* (1996).
2. North American Symptomatic Carotid endarterectomy Trial (NASCEF) Steering Committee, "North American symptomatic carotid endarterectomy trial: methods, patient characteristics and progress," *Stroke*, 22:711-720, 1991.
3. M. Kass, A. Witkin, and D. Terzopoulos, "Snake: active contour models," *Int.J.Comp.Vision*, Vol.1, pp.312-331, 1988.
4. Françoise Lefebvre, Geneviève Berger, and Pascal Laugier. Automatic Detection of the Boundary of the Calcaneous from Ultrasound Parametric Images Using an Active Contour Model; Clinical Assessment. *IEEE Trans. Med.Imaging*. Vol.17, No.1, pp45-52, 1998.
5. T.D.Jones and P.Plassmann. An Active Contour Model for Measuring the Area of Leg Ulcers. *IEEE Trans.Med.Imaging*. Vol 19, No.12 1202-1210,2000
6. V.J.Miller, E.D.Breen, E.W.Lorensen and et. al. Geometrically deformed models: a method for extracting closed geometric models from volume data. Proc. Computer Graphics SIGGRAPH' 91 Conf. (Las Vegas, NV) vol 25, pp217-226, 1991.
7. S. Lobregt and A.M.Viergever. A discrete dynamic contour model. *IEEE Trans.Med.imaging*. Vol.14 12-24, 1995.
8. Abir Zahalka and Aaron Fenster. An automated segmentation method for three-dimensional carotid ultrasound images. *Physics in Medicine and Biology*. Vol.46, 1321-1342, 2001.
9. Xiaolan Zeng, Lawrence H.staib, Robert T. Schulz and James S.Duncan. Segmentation and Measurement of the Cortex from 3-D MR Images Using Coupled-Surfaces Propagation. *IEEE Trans. Med. Imaging*. Vol.18, No.10, 927-937, 1999.
10. Yusuf Sinan Akgul, Chandra Kambhamettu, and Maureen Stone. "Automatic Extraction and Tracking of the Tongue Contours", *IEEE Trans. Med. Imaging*. Vol.18, No.10, 1035-1045, 1999.